

A Robust Cohesive Zone Model for Cyclic Loading

Ala Tabiei and Wenlong Zhang
Department of Mechanical Engineering
University of Cincinnati, Cincinnati, OH 45221-0070

Abstract

Cohesive element approach is a promising way to simulate crack propagation. Commonly used cohesive laws include bilinear law, trapezoidal law and exponential law. However, research has found that when exponential cohesive law is unloading or reloading, the traction curve cannot remain continuous when the mixed mode ratio changes. (Kregting 2005) [1] In this paper, the discontinuity behavior of exponential law is discussed and a remedy is given to handle that. Instead of using a constant unloading slope, we use an unloading and reloading slope that changes with mixed mode ratio, like the damage parameter used in bilinear model. Improved Xu-Needleman's exponential cohesive law will be used as an example to show this improvement. Its application in cyclic loading for fatigue failure is presented.

Keywords: Cohesive zone model; Improved Xu-Needleman cohesive law; Bilinear cohesive law; Unloading behavior; Reloading behavior; Continuity; Cyclic loading

Introduction

The concept of cohesive zone, firstly conceived by Dugdale (1960) [2] and Barenblatt (1962) [3], is used to handle the process zone ahead of crack tip that linear elastic fracture mechanics (LEFM) doesn't work well when the process zone is not sufficiently small compared to the structural size. It treats the process zone as a cohesive zone in which there exists traction between two virtual surfaces ahead of the crack tip and it degrades as the separation between the surfaces increases, and when the traction decrease to zero, the virtual surfaces are considered to form real crack surfaces. The area under the traction separation curve is the energy consumed to open the surfaces, thus connected with physical model. This method is straightforward and powerful. It can be used to handle fracture problems whose geometry has or doesn't have initial cracks (or blunt crack), and the latter one is hard to do in LEFM.

In 1976, Hillerborg [4] first applied cohesive zone model in finite element method to simulation crack initiation and growth in concrete beam. In 1994 Xu and Needleman [5] first inserted cohesive interface elements to every element interface to allow arbitrary dynamic crack propagation and produced good results. These cohesive interface elements have zero thickness and are inserted prior to the beginning of simulation, and it's called intrinsic approach. The success of Xu and Needleman brought an encouraging insight into the fracture simulation that crack propagation can be simulated in a much easier way where no complicated failure criteria and topologies but only the information of cohesive zone model is needed. Similar to Xu and Needleman, Ortiz (1999) [6] used zero thickness cohesive element in a way that instead of having cohesive interface elements at the beginning of simulation, they are inserted progressively to locations where certain criterion is met, like stress reaching material strength and this is referred to as extrinsic approach. There are other ways to imbed cohesive zone models into fracture simulations, like using Partition of Unity Method (PUM) in Extended Finite Element Method [7], or smeared crack approach [8].

Large attention has been put on cohesive traction separation law (TSL) since it is the only information controls the cohesive zone model behavior. Various TSLs are proposed by different people, the biggest different between these TSLs is the shape. The most common shapes are bilinear (Camanho 2003) [9], exponential (Xu 1993)[5], and trapezoidal (Tvergaard V, Hutchinson 1992) [10]. Although the shape of TSL are different, they all have common features that the area under the traction-separation curve represents the critical energy release rate, and the maximum traction represents the maximum tensile or shear strength in the material. Different studies have been carried out on the influence of cohesive law shape on the simulation result. K. Volokh 2004 [11] used different cohesive laws on a block peel test and showed the shape of cohesive zone model is important. Giulio Alfano 2005 [12] conducted a comprehensive study and concluded that for a typical double cantilever beam test the solution is practically independent from the shape of cohesive law, whereas up to 15% difference in the maximum load is recorded in a rigid compact specimen.

Among these various cohesive models we are especially interested in the exponential cohesive model since we observed some discontinuity in the traction curve as it unloads or reloads in a different mixed mode ratio, and it will be elaborated in detail in section.

A cohesive law is called irreversible if it considers damage accumulation and its unloading path don't follow the same loading path. When irreversible cohesive law is used, an unloading and reloading path needs to be defined to determine the unloading and reloading behavior. In this paper, bilinear and exponential cohesive law's traction separation law will be briefly reviewed and then their unloading and reloading behavior will be examined. A discontinuous behavior during the reloading process of exponential law is observed (Figure 1) when it's reloading at a different mixed mode ratio. The mixed mode ratio we used in this paper is the ratio between tangential separation rate and normal separation rate:

$$r = \frac{\dot{\Delta}_t}{\dot{\Delta}_n}$$

Two conditions in combination caused this discontinuity behavior: (1) Unloading and reloading behavior is described using a constant slope, and this is what commonly used in literature [13-15]. (2) The mixed mode ratio r changes during the unloading or reloading process.

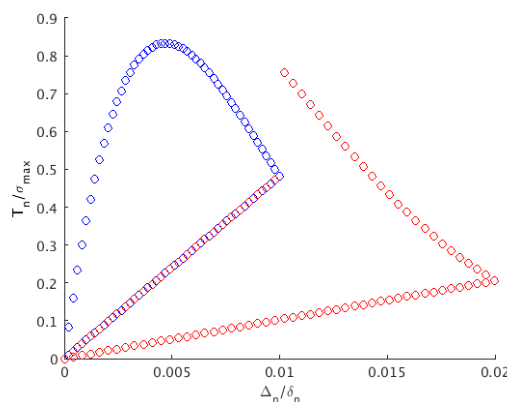


Figure 1: Discontinuity in Improved Xu-Needleman's model when reload at different mixed mode ratio using constant unloading/reloading slope

Bilinear cohesive law and its unloading and reloading behavior

We will start by looking at a bilinear cohesive law by Camanho (2003) [9]. It is formulated based on damage mechanics and B-K (1997) mixed mode criterion [16] and was implemented in LS-DYNA[®]'s material library as MAT_138 [17]. In bilinear cohesive law, it considers the mixed mode separation (Equation 1) as an input and uses it to calculate the damage parameter (Equation 2), which is incorporated in the expression of traction separation relationship:

$$\delta = \sqrt{\delta_1^2 + \delta_2^2 + \langle \delta_3^2 \rangle} \quad (1)$$

Where δ_1 and δ_2 corresponds to the in plane shear separation; δ_3 is the normal separation and is taken as 0 when it's negative. $\langle x \rangle$ is the Macaulay bracket:

$$\langle x \rangle = \begin{cases} x & \text{if } x > 0 \\ 0 & \text{if } x \leq 0 \end{cases} \quad (2)$$

The damage parameter is:

$$D = \min \left(\frac{\delta^F}{\delta_{max}} \frac{\delta_{max} - \delta^0}{\delta^F - \delta^0}, 1 \right) \quad (3)$$

Where δ^0 (Equation 4) is the mixed mode separation corresponding to maximum traction, it corresponds to the point when damage initiates. δ^F (Equation 5) is the mixed mode failure separation, exceeding which the cohesive element will be considered failed and deleted. δ_{max} records the history of mixed mode separation δ and takes the largest positive separation in history. In this way the damage parameter cannot decrease and this is how the irreversible behavior is controlled. The damage parameter ranges from 0 to 1 and when it reaches 1 the cohesive element is considered totally damaged and not able to carry any more load.

$$\delta^0 = \delta_I^0 \delta_{II}^0 \sqrt{\frac{1 + \beta^2}{(\delta_{II}^0)^2 + (\beta \delta_I^0)^2}} \quad (4)$$

$$\delta^F = \begin{cases} \frac{2(1 + \beta^2)}{\delta^0} \left[\left(\frac{EN}{G_{IC}} \right)^\alpha + \left(\frac{ET\beta^2}{G_{IIC}} \right)^\alpha \right]^{-1/\alpha} & \delta_3 > 0 \\ \frac{2G_{IIC}}{S} & \delta_3 \leq 0 \end{cases} \quad (5)$$

In these equations, $\delta_I = \delta_3$ and $\delta_{II} = \sqrt{\delta_1^2 + \delta_2^2}$; $\beta = \delta_{II}/\delta_I$, α is parameter determined by user. After all the damage parameter is define, the traction can be expressed as:

$$\text{Normal separation:} \quad T = \begin{cases} E \times (1 - D) \times \delta_3 & 0 < \delta_3 < \delta^F \\ E \times \text{Scale Factor} \times \delta_3 & \delta_3 < 0 \end{cases} \quad (6)$$

$$\text{Tangential separation:} \quad S = G \times (1 - D) \times \delta_1 \text{ (or } \delta_2) \quad (7)$$

Where E and G are elastic and shear modulus in cohesive law, and they are usually taken as a much higher value than the elastic modulus of bulk material to minimize the extra compliance.

The way the damage parameter is formulated in bilinear model makes it incorporate the mixed mode behavior thus no matter how the mixed mode ratio changes, the bilinear cohesive law can always remain continuous. As an example, a 3D and 2D plot is given in Figure 2, in the first cycle of loading, the mixed mode ratio is $r = 1$; in the reloading cycle, mixed mode ratio changes to $r = 1/16$.

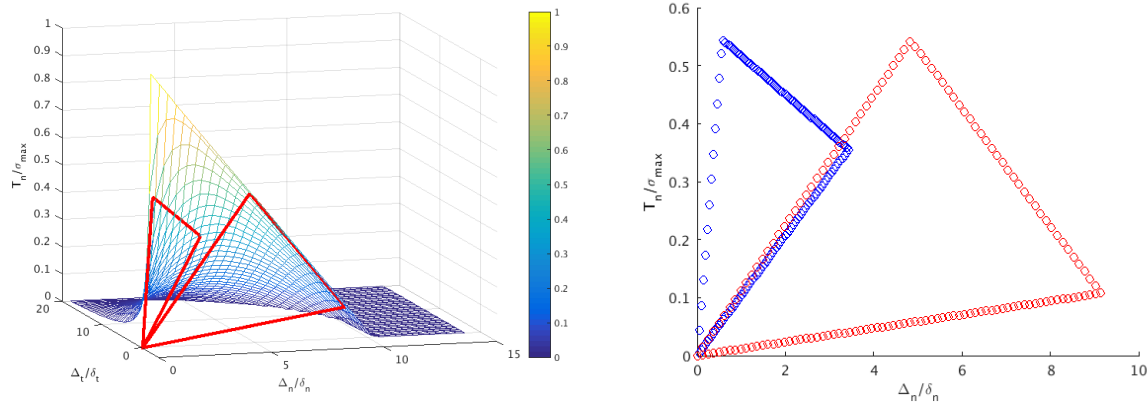


Figure 2: Continuous behavior of bilinear cohesive law during unloading and reloading process when mixed mode ratio changes

Exponential cohesive law and its discontinuity during unloading and reloading process

The exponential cohesive law proposed by Xu and Needleman (1994) [5] was formed potential based. For exponential cohesive law, however, the damage parameter usually used in literature is not closely related to mixed mode separation. In this paper an improved Xu-Needleman’s cohesive law is adopted as an example. It is proposed by (Bosch 2006) [18] to address the energy inconsistency in the mixed mode decohesion process. The energy consistency is tested by separating the cohesive element in normal direction first for a certain distance Δ_n before failure, then separate in the tangential direction till failure. The normal and tangential energy versus normal displacement in the first step is plotted in Figure 3 (a). And we can see in the improved exponential cohesive model the total energy is constant no matter how Δ_n changes. This is not the case in the bilinear model (Figure 3 (b)).

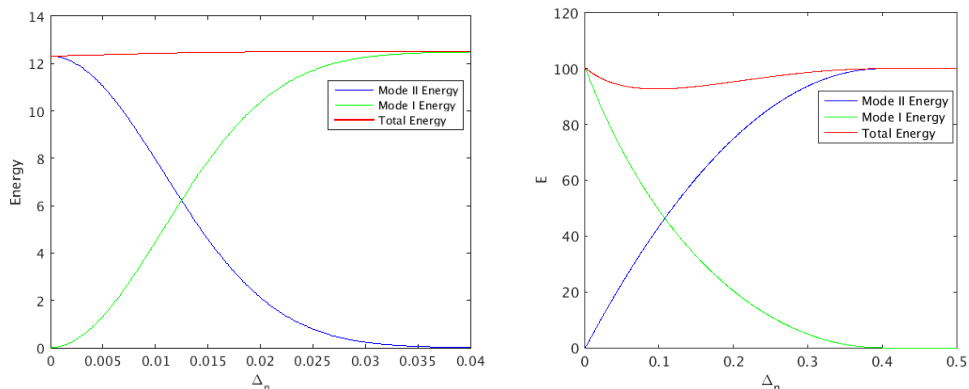


Figure 3: (a) Energy consistency of improved exponential cohesive model; (b) Energy inconsistency of bilinear cohesive model

The modified Xu-Needleman's cohesive law has the following form:

$$\phi(\Delta_n, \Delta_t) = \phi_n \left[1 - \left(1 + \frac{\Delta_n}{\delta_n} \right) \exp\left(-\frac{\Delta_n}{\delta_n}\right) \exp\left(-\frac{\Delta_t^2}{\delta_t^2}\right) \right] \quad (8)$$

$$T_n = \frac{\partial \phi}{\partial \Delta_n} = \frac{\phi_n}{\delta_n} \left(\frac{\Delta_n}{\delta_n} \right) \exp\left(-\frac{\Delta_n}{\delta_n}\right) \exp\left(-\frac{\Delta_t^2}{\delta_t^2}\right) \quad (9)$$

$$T_t = \frac{\partial \phi}{\partial \Delta_t} = 2 \frac{\phi_t}{\delta_t} \left(\frac{\Delta_t}{\delta_t} \right) \left(1 + \frac{\Delta_n}{\delta_n} \right) \exp\left(-\frac{\Delta_n}{\delta_n}\right) \exp\left(-\frac{\Delta_t^2}{\delta_t^2}\right) \quad (10)$$

Where $\delta_n = \phi_n/(eT_n)$, and $\delta_t = \phi_t/(T_n\sqrt{e/2})$. Park (2011) [44] stated that potential based models proposed under the condition of monotonic separation path needs independent unloading and reloading relations. The unloading and reloading behavior of the improved Xu-Needleman cohesive law is usually did by linear interpolation, like in paper of Kullari 2014 [15]. When cohesive zone starts to unload, a ratio between the traction and separation at that point is calculated and used as the unloading and reloading slope. The damage parameter in normal and tangential direction is given as:

$$d_n = 1 - \exp\left(-\frac{\Delta_{n,max}}{\delta_n}\right) \exp\left(-\frac{\Delta_{t,max}^2}{2\delta_t^2}\right) \quad (11)$$

$$d_t = 1 - \exp\left(-\frac{\Delta_{t,max}^2}{2\delta_t^2}\right) \exp\left(-\frac{\Delta_{n,max}}{\delta_n}\right) \left(1 + \frac{\Delta_{n,max}}{\delta_n} \right) \quad (12)$$

And traction during the unloading and reloading process is calculated by using:

$$\begin{cases} T_n = (1 - d_n)K_n\Delta_n \\ T_t = (1 - d_t)K_t\Delta_t \end{cases} \quad (13)$$

Where $K_n = G_{IC}/\delta_n^2 = e^2T_n^2/G_{IC}$ and $K_t = 2G_{IIC}/\delta_t^2 = eT_t^2/G_{IIC}$ are the initial slope of the cohesive law in normal and tangential direction. This works fine when mixed mode ratio doesn't change during the process, as shown in Figure 4.

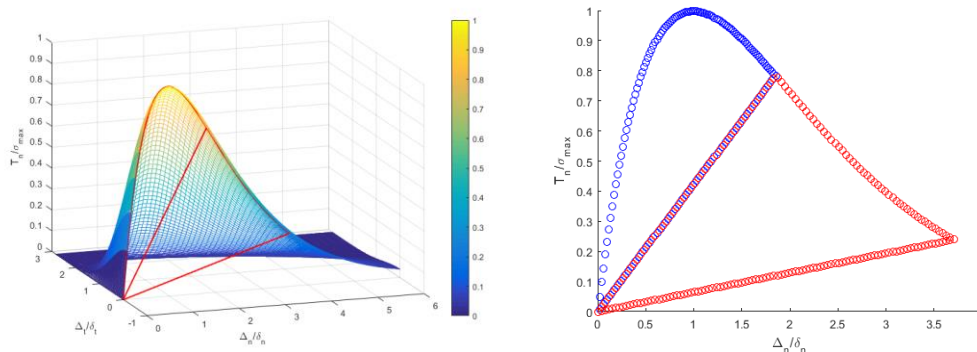


Figure 4: Linear interpolation for unloading and reloading behavior of improved exponential law when the mixed mode ratio doesn't change

However, when mixed mode ratio changes, for example, from $r = 1$ in the first load cycle to $r = 0.5$ in the second load cycle, the traction curve cannot remain continuous, like in Figure 5. This is because unlike the damage parameter in bilinear law, which is constantly updating with mixed mode ratio through δ_{max} , δ_0 and δ_F , the interpolation based slope for exponential law can only consider the mixed mode state when it start to unload.

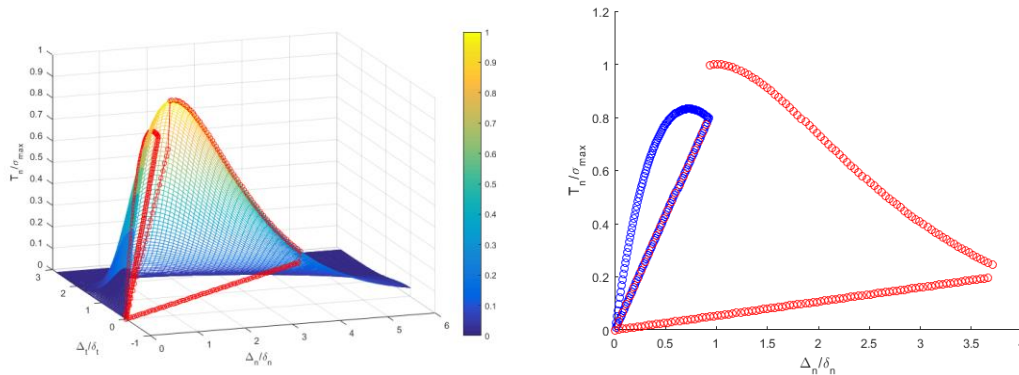


Figure 5: Discontinuity during unloading and reloading process of improved exponential law using constant slope when the mixed mode ratio changes

The consequence of this discontinuity is not yet discussed in literature to the best of author's knowledge, but such discontinuity is for sure undesirable in numerical simulation and could possibly cause some numerical instabilities. For crack propagation problems, where unloading and reloading is likely to happen as energy keeps being released at the crack tip; For fatigue simulation where millions of cycles of reloading happen, it is possible that the mixed mode ratio changes during this process. So it is important to guarantee a continuous and robust unloading and reloading behavior of the cohesive law.

Remedies to fix the discontinuity in unloading and reloading process of exponential cohesive law when mixed mode ratio changes

Kregting in 2005 [1] has talk about this discontinuity and tried to solve it using extrapolation to update the constant slope in the new load cycle. His remedy is based on an assumption that mixed mode ratio doesn't change within a load cycle. When the cohesive element starts to unload, the mixed mode separation Δ_{cycle1} is recorded and the corresponding tangential separation Δ_t and normal separation Δ_n are used to calculate the unloading slope. When a new loading cycle starts, the mixed mode ratio r for that cycle is captured and extrapolation is did to find a new pair of tangential and normal separation Δ_t, Δ_n that will reach the mixed mode separation Δ_{cycle1} of the first cycle. And this new pair of separations is used to calculate the new reloading slope. It works well when mixed mode ratio is constant within one loading cycle (Figure 6).

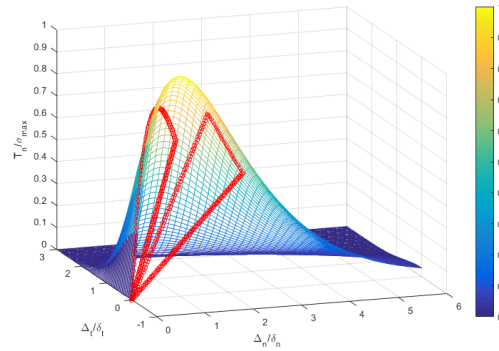


Figure 6: Reloading behavior using Rene’s extrapolation method when mixed mode ratio is constant within a cycle

However, when the mixed mode ratio changes during reloading period, for example it first reloads following $r = 1$ then changes to $r = 2$ before it reaches maximum separation Δ_{max} of last cycle, the curve can no longer be continuous using Rene’s extrapolation method because the unloading and reloading slope using this method is constant within one loading cycle thus cannot capture that change (Figure 7).

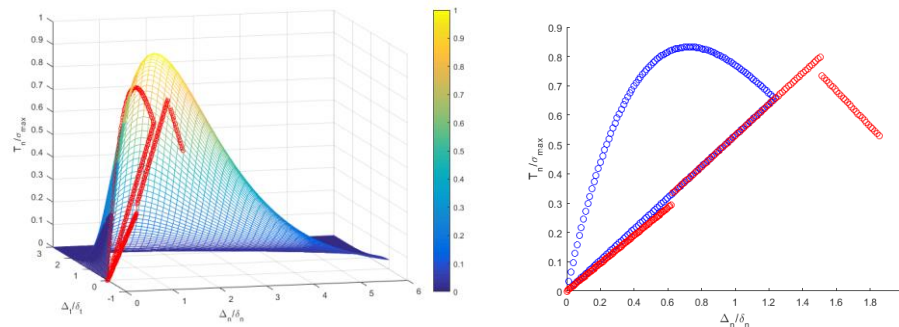


Figure 7: Discontinuity in exponential cohesive law using extrapolation method when mixed mode ratio changes within a load cycle

To fix that a new continuous damage parameter that considers the mixed mode ratio change is proposed in this paper. The idea is to release the tangential separation in damage factor for normal traction, and release the normal separation in damage factor for tangential traction (Equation 14, 15).

$$d_n = \exp\left(-\frac{\Delta_{n,max}}{\delta_n}\right) \exp\left(-\frac{\Delta_t^2}{2\delta_t^2}\right) \tag{14}$$

$$d_t = \exp\left(-\frac{\Delta_{t,max}^2}{2\delta_t^2}\right) \exp\left(-\frac{\Delta_n}{\delta_n}\right) \left(1 + \frac{\Delta_n}{\delta_n}\right) \tag{15}$$

Where $\Delta_{n,max}$ and $\Delta_{t,max}$ are defined as:

$$\Delta_{n,max} = \sqrt{\Delta_{max}^2 - \Delta_t^2} \tag{16}$$

$$\Delta_{t,max} = \sqrt{\Delta_{max}^2 - \Delta_n^2} \tag{17}$$

In this way, the mixed mode interaction is considered for both the unloading, reloading slope and the point on max separation envelop of last cycle. Then the traction will be calculated using the same equation:

$$\begin{cases} T_n = d_n K_n \Delta_n \\ T_t = d_t K_t \Delta_t \end{cases} \text{ when } \Delta_m \leq \Delta_{m,max} \tag{18}$$

When $\Delta_m = \sqrt{\Delta_n^2 + \Delta_t^2}$ reaches the separation envelope again, the traction separation relationship will follow the improved exponential cohesive law again and $\Delta_{m,max}$ will increase correspondingly. Using the new damage parameter helps remain the continuity of cohesive law no matter what loading and unloading path is like, as shown in Figure 8, in which the mixed mode ratio changed during the reloading period. Note bilinear cohesive model also has the capability to remain continuous even when mixed mode ratio changes within one load cycle.

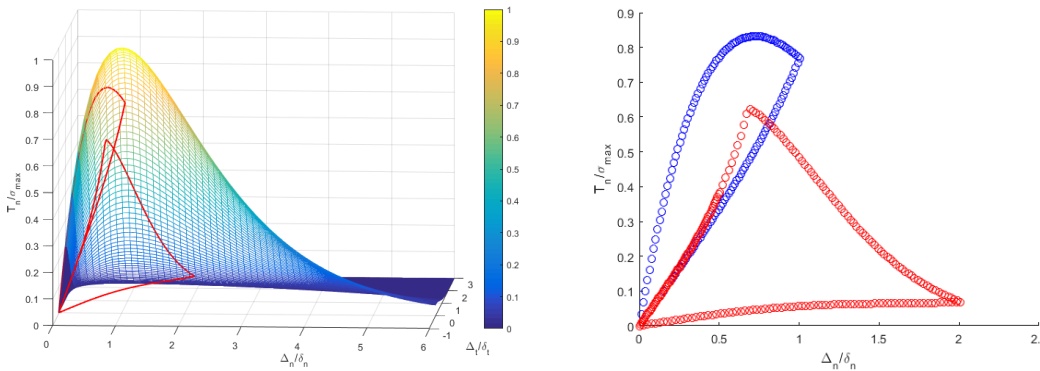


Figure 8: Continuity in exponential cohesive law using proposed unloading and reloading method when mixed mode ratio changes within a load cycle

Implementation of the cohesive zone model to interface fatigue crack growth

CZM has been used on fatigue prediction by different authors. ([19][20]) Roe 2003 [13] adopted Xu-Needleman’s exponential cohesive model for cyclic loading fatigue analysis. His model incorporated typical damage evolution laws: (1) damage only starts to accumulate if a deformation is greater than a critical magnitude; (2) The increment of damage is related to the increment of deformation at the current load level; (3) There exist an endurance limit the stress below which can proceed cyclically without producing failure. Based on these three requirements he gave the evolution equation:

$$\dot{D}_c = \frac{|\dot{\Delta}|}{\delta_{\Sigma}} \left[\frac{\bar{T}}{\sigma_{max}} - C_f \right] H(\Delta - \delta_0) \text{ and } \dot{D}_c \geq 0 \tag{19}$$

Where H is Heaviside function. The present damage evolution law is formulated using effective cohesive zone quantities. The resultant separation, Δ , and its increment are defined as:

$$\Delta = \sqrt{\Delta_n^2 + \Delta_t^2}, \quad \dot{\Delta} = \Delta_t - \Delta_{t-\Delta t} \quad (20)$$

The result traction, \bar{T} is defined as:

$$\bar{T} = \sqrt{T^2 + S^2} \quad (21)$$

A new parameter called cohesive zone endurance limit σ_f is incorporated via C_f , the ratio of σ_f and the initial undamaged cohesive normal strength:

$$C_f = \frac{\sigma_f}{\sigma_{max,0}}, \quad 0.0 < C_f < 1.0 \quad (22)$$

After the damage rate is calculated, the current cohesive strength is then scale down by

$$\sigma_{max} = \sigma_{max,0}(1 - D), \quad \tau_{max} = \tau_{max,0}(1 - D), \quad (23)$$

During the unloading and reloading process where the current separation is smaller than the largest value of last cycle, the traction is calculated by

$$T_n = T_{n,max} + k_n(\Delta u_n - \Delta u_{n,max}) \quad (24)$$

$$T_t = T_{t,max} + k_t(\Delta u_t - \Delta u_{t,max}) \quad (25)$$

Where k_n , k_t used in Roe's paper are constant values. In this paper that constant slope is replaced by a parameter that changes with mixed mode ratio to account for mixed mode ratio change between each loading cycles. An example is carried out to show schematically how our unloading and reloading methodology of exponential cohesive law help the continuity of the cohesive law. Make the tangential and normal separation change cyclically and in such a way that the mixed mode ratio changes between each cycle (Figure 9). Using constant unload and reload slope, we can see it the discontinuity in the cohesive law is very obvious (Figure 10 (a)). However, for our proposed unloading and reloading methodology, the cohesive law remains continuous very well (Figure 10 (b)). Another verification is done by making the separation a function of $|\sin(t)|$, like shown in figure 11. Again constant unloading slope (Figure 12 (a)) shows discontinuity and our proposed method is not (Figure 12 (b)).

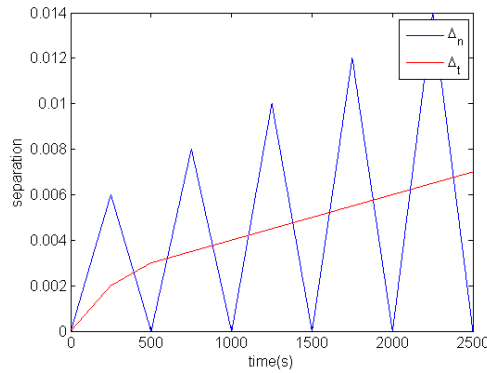


Figure 9: Cyclic separation history in cohesive model

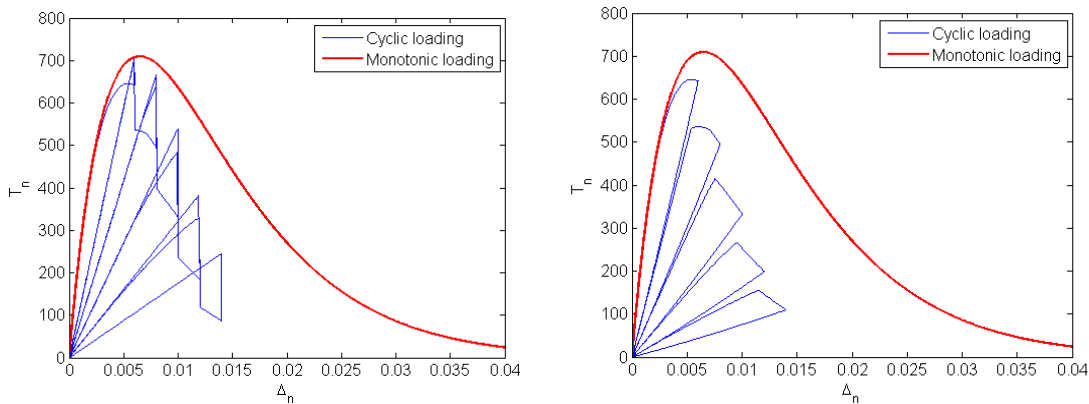


Figure 10: (a) Cyclic loading of exponential cohesive law using constant unloading and reloading slope (b) Cyclic loading of exponential cohesive law using proposed unloading and reloading methodology

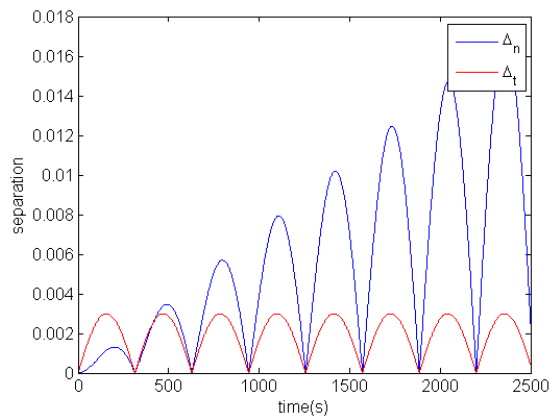


Figure 11: Cyclic separation history in cohesive model

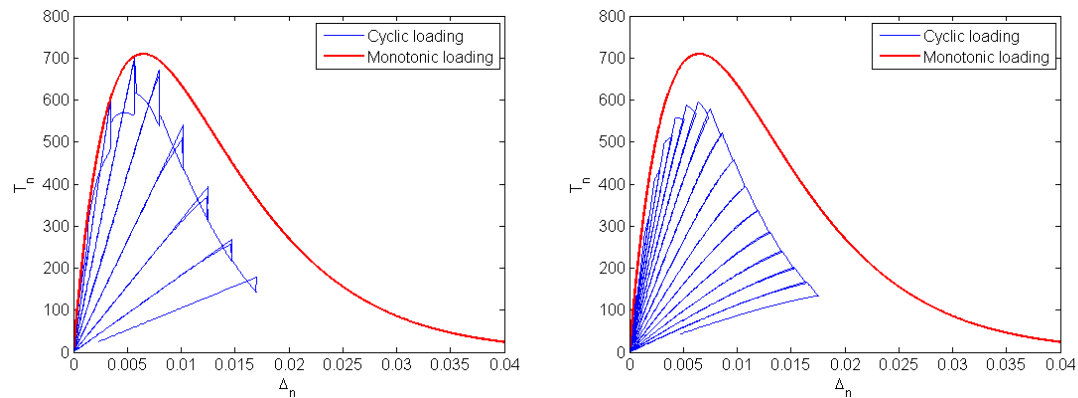


Figure 12: (a) Cyclic loading of exponential cohesive law using constant unloading and reloading slope (b) Cyclic loading of exponential cohesive law using proposed unloading and reloading methodology

Conclusion

In this paper a brief review of cohesive zone model is carried out, and the unloading and reloading behavior of bilinear and exponential law is analyzed. It's found that the commonly used constant unloading slope method for exponential law could lead to discontinuity when the mixed mode ratio changes. Thus a new methodology for unloading and reloading behavior of exponential law is proposed and verified on fatigue cyclic loading using two different loading histories. The result proves its ability to retain continuity under arbitrary load and unload history that constant unloading slope method couldn't have.

References

- [1] Kregting R. Cohesive zone models: Towards a robust implementation of irreversible behaviour. Philips Applied Technologies 2005.
- [2] Dugdale D. Yielding of steel sheets containing slits. *J Mech Phys Solids* 1960;8:100-4.
- [3] Barenblatt GI. The mathematical theory of equilibrium cracks in brittle fracture. *Adv Appl Mech* 1962;7:55-129.
- [4] Hillerborg A, Mod er M, Petersson P. Analysis of crack formation and crack growth in concrete by means of fracture mechanics and finite elements. *Cem Concr Res* 1976;6:773-81.
- [5] Xu X, Needleman A. Numerical simulations of fast crack growth in brittle solids. *J Mech Phys Solids* 1994;42:1397-434.
- [6] Ortiz M, Pandolfi A. Finite-deformation irreversible cohesive elements for three-dimensional crack-propagation analysis. *Int J Numer Methods Eng* 1999;44:1267-82.
- [7] Wells G, Sluys L. A new method for modelling cohesive cracks using finite elements. *Int J Numer Methods Eng* 2001;50:2667-82.
- [8] Borst Rd, Remmers JJ, Needleman A, Abellan M. Discrete vs smeared crack models for concrete fracture: bridging the gap. *Int J Numer Anal Methods Geomech* 2004;28:583-607.
- [9] Camanho PP, Davila C, De Moura M. Numerical simulation of mixed-mode progressive delamination in composite materials. *J Composite Mater* 2003;37:1415-38.
- [10] Tvergaard V, Hutchinson JW. The influence of plasticity on mixed mode interface toughness. *J Mech Phys Solids* 1993;41:1119-35.
- [11] Volokh KY. Comparison between cohesive zone models. *Communications in Numerical Methods in Engineering* 2004;20:845-56.
- [12] Alfano G. On the influence of the shape of the interface law on the application of cohesive-zone models. *Composites Sci Technol* 2006;66:723-30.
- [13] Roe K, Siegmund T. An irreversible cohesive zone model for interface fatigue crack growth simulation. *Eng Fract Mech* 2003;70:209-32.

- [14] Nguyen O, Repetto E, Ortiz M, Radovitzky R. A cohesive model of fatigue crack growth. *Int J Fract* 2001;110:351-69.
- [15] Kolluri M, Hoefnagels J, van Dommelen J, Geers M. Irreversible mixed mode interface delamination using a combined damage-plasticity cohesive zone enabling unloading. *Int J Fract* 2014;185:77-95.
- [16] Benzeggagh M, Kenane M. Measurement of mixed-mode delamination fracture toughness of unidirectional glass/epoxy composites with mixed-mode bending apparatus. *Composites Sci Technol* 1996;56:439-49.
- [17] LSDYNA keyword user's manual, volume II, material models. 2013.
- [18] Van den Bosch M, Schreurs P, Geers M. An improved description of the exponential Xu and Needleman cohesive zone law for mixed-mode decohesion. *Eng Fract Mech* 2006;73:1220-34.
- [19] Bouvard J, Chaboche J, Feyel F, Gallerneau F. A cohesive zone model for fatigue and creep-fatigue crack growth in single crystal superalloys. *Int J Fatigue* 2009;31:868-79.
- [20] Turon A, Costa J, Camanho P, Dávila C. Simulation of delamination in composites under high-cycle fatigue. *Composites Part A: applied science and manufacturing* 2007;38:2270-82.